




Large eddy simulation of wind farm performance in horizontally and vertically staggered layouts

Muhammad Rubayat Bin Shahadat^{a,b}, Mohammad Hossein Doranehgard^{a,b,*}, Weibing Cai^a, Zheng Li^{a,**} 

^a Department of Mechatronics Engineering, Morgan State University, Baltimore, MD, 21251, USA

^b Department of Mechanical Engineering, Johns Hopkins University, Baltimore, MD, 21218, USA

ARTICLE INFO

Keywords:

Wind farm
LES
ADM
Vertical and horizontal staggering
Power generation efficiency

ABSTRACT

This numerical investigation employs Large Eddy Simulation (LES) coupled with Actuator Disk Model (ADM) to evaluate wind farm layout optimization strategies. The study presents a systematic analysis of aligned, horizontal staggering, vertical staggering, and mixed (combination of horizontal and vertical) staggering configurations, aiming to establish optimal design parameters for enhanced power production. The investigation examines key performance metrics including mean velocity distributions, turbulence intensity characteristics, and power generation efficiency. Results demonstrate better performance of both horizontal and vertical staggering patterns compared to conventional aligned configurations, with horizontal staggering exhibiting notably higher power output than vertical arrangements. Our findings also suggest that mixed configurations, incorporating both horizontal and vertical staggering, can offer optimal performance characteristics. This research advances the understanding of wake interactions in complex wind farm layouts and provides design guidelines for maximizing wind farm power generation efficiency through strategic turbine positioning.

1. Introduction

1.1. Background

Wind energy has emerged as a vital element in the global energy transition, motivated by two key imperatives: climate change mitigation and reduced dependence on limited fossil fuel resources [1,2]. As a renewable energy source, wind power offers abundance, scalability, and growing cost advantages compared to conventional energy sources [3–6]. The International Renewable Energy Agency (IRENA) reports that global installed wind energy capacity experienced exponential growth in the past decade, attaining 837 GW in 2022. Current projections indicate wind power will play a crucial role in reaching net-zero emissions targets by 2050 [7].

Modern wind farms feature groups of strategically positioned turbines that capture high-altitude wind flows and convert kinetic energy to electricity [8]. Deploying large-scale wind farms, whether on land or at sea, requires optimization of design and operational factors to

enhance efficiency while reducing costs [9,10]. A major operational challenge lies in the wake effect—where upstream turbines create zones of reduced wind speed and heightened turbulence. These wakes diminish the performance of downstream turbines, resulting in significant power reduction [11–13]. Previous research studies [14–16] show that wake-related losses may reach up to 20 % of a wind farm's total energy output, highlighting the need to understand and address these effects.

Progress in numerical modeling and experimental research has transformed how we analyze wind farm dynamics. Based on these advancements, recent studies [17–22] have investigated wind resource assessment, reactive power dispatch, and optimal power flow to support the integration of renewable energy into power systems. Researchers have applied multi-objective optimization techniques to achieve cost-effective generation, employed stochastic algorithms to address uncertainties in wind and solar power generation, and used probabilistic methods to evaluate wind potential across diverse regions. Collectively, these studies underscore the importance of optimizing power generation

This article is part of a special issue entitled: SpliTech2024 published in Energy.

* Corresponding author. Department of Mechatronics Engineering, Morgan State University, Baltimore, MD, 21251, USA.

** Corresponding author.

E-mail addresses: mohammad.doranehgard@morgan.edu (M.H. Doranehgard), zheng.li@morgan.edu (Z. Li).

<https://doi.org/10.1016/j.energy.2025.135569>

Received 30 December 2024; Received in revised form 26 February 2025; Accepted 10 March 2025

Available online 11 March 2025

0360-5442/© 2025 Published by Elsevier Ltd.

while accounting for resource variability and setting the scope for further investigation of wind farm configurations that can enhance energy capture and efficiency. Large Eddy Simulations (LES) now serve as the foundation for precise numerical studies, allowing researchers to unravel complex turbulent interactions between turbines and the atmospheric boundary layer (ABL) [23–25]. Experimental methods, such as scaled wind tunnel testing and field measurements, enhance numerical studies through validation and physical understanding [26]. Research by Chamorro and Porté-Agel [27] demonstrates how wind tunnel studies effectively capture wake interactions in both aligned and staggered turbine arrangements. This combined approach showcases the productive partnership between computational and experimental methods in improving wind farm design and operation.

The spatial arrangement or layout of turbines within a wind farm is one of the most crucial factors influencing overall performance. The layout determines the extent of wake interactions and, consequently, the farm's energy yield and operational reliability [28]. Optimizing wind farm layouts involves balancing turbine density and inter-turbine spacing to maximize energy production while minimizing wake losses and maintenance costs. Horizontal arrangements of turbines, such as aligned and staggered configurations, have been extensively studied [29,30]. Aligned layouts, where turbines are placed in straight rows perpendicular to the prevailing wind direction, are straightforward to implement but often result in significant wake overlap, reducing downstream power production [31,32]. In contrast, staggered layouts, where turbines are offset in successive rows, have shown improved performance by promoting wake recovery and reducing overlap [33]. In this context, Stevens et al. [34] using LES revealed that staggered configurations achieve better vertical mixing and kinetic energy flux compared to aligned layouts, resulting in higher power production in the fully developed region of the wind farm.

Despite the improvement of research on horizontal layouts, vertical staggering remains an underexplored concept. Vertical staggering involves varying the hub heights of turbines in consecutive rows to leverage the velocity gradients within the ABL. Initial studies, such as that done by Zhang et al. [35], suggest that vertical staggering can significantly improve power production in the entrance region of wind farms by reducing wake interactions. However, its effectiveness in the fully developed regime remains ambiguous due to the lack of substantial vertical kinetic energy flux enhancements. The potential benefits and trade-offs of vertical staggering need further investigation to determine its viability as a design strategy for future wind farms.

Numerical modeling tools have been indispensable in advancing wind farm design and operation by providing insights into wake dynamics, turbine interactions, and layout optimization. Among these tools, the Actuator Line Model (ALM) and the Actuator Disk Model (ADM) are widely used for simulating wind farm flows [36–39]. The ALM is a high-fidelity approach that represents turbine blades as rotating lines, capturing the aerodynamic forces and resulting wake structures in detail. This model is particularly effective in studying near-wake phenomena, blade-specific dynamics, and turbine control strategies [40,41]. However, the ALM's computational demands make it less practical for simulating large wind farms, where the focus is often on far-wake interactions and overall farm performance [42]. Studies such as that done by Troldborg et al. [43] highlighted the ALM's accuracy in resolving wake dynamics while emphasizing its limitations in scalability for extensive simulations.

On the other hand, the ADM simplifies turbines as stationary disks that uniformly extract momentum from the incoming flow. While this approach sacrifices some accuracy in near-wake predictions, it significantly reduces computational costs, making it ideal for large-scale simulations [44–46]. Importantly, this trade-off in accuracy is minimal when the primary objective is to study far-wake interactions and overall wind farm performance. The ADM has been extensively validated against experimental data, with studies such as that done by Stevens et al. [34] demonstrating its efficacy in capturing far-wake behavior and

overall wind farm dynamics. Additionally, the ADM's compatibility with LES frameworks allows researchers to investigate complex interactions between turbine arrays and the ABL under various atmospheric conditions [47]. This capability is particularly critical for studying vertically and mixed staggered layouts, where vertical wind shear and wake recovery dynamics play a central role.

Given the study's focus on optimizing wind farm layouts to reduce wake interference and enhance power generation, the ADM is chosen for its computational efficiency and scalability. Investigating both horizontally and vertically staggered configurations requires simulating large turbine arrays over extended domains, where the ADM's faster runtime enables comprehensive parametric studies without compromising the fidelity needed to capture far-wake behavior. Furthermore, employing ADM with LES provides sufficient accuracy to analyze the key factors influencing wind farm performance, such as wake recovery, turbulence intensity, inter-turbine spacing, and power generation. Thus, the ADM represents the optimal balance between computational feasibility and accuracy, ensuring that the findings are both reliable and applicable to real-world wind farm design.

This study aims to address the existing gaps in wind farm layout optimization by systematically investigating horizontally and vertically staggered configurations using the ADM framework. Horizontally staggered layouts, which offset turbines in successive rows, are well-established as a means to enhance wake recovery and reduce power losses. In contrast, vertically staggered layouts, which vary turbine heights, offer a novel approach to exploiting the vertical wind shear within the ABL. Despite their potential, vertically staggered layouts have received limited attention in the literature, leaving their effectiveness and applicability largely unexplored.

By employing LES with the ADM, we will analyze the aerodynamic and energetic impacts of these configurations under various operating conditions. This work seeks to provide a comprehensive assessment of horizontally and vertically staggered layouts, contributing to the development of optimized wind farm designs that maximize energy yield while minimizing costs and wake-induced losses. The findings are expected to offer valuable insights for the wind energy industry and guide future research directions in wind farm layout optimization.

1.2. Research gap and the novelty

While extensive research has explored horizontally staggered configurations for wind farm layout optimization, vertical staggering remains largely unexplored. The limited studies addressing vertical staggering have primarily focused on isolated aspects, leaving significant knowledge gaps. Furthermore, the literature lacks comprehensive analyses of mixed configurations that combine both horizontal and vertical staggering approaches. This study presents the first systematic investigation of such mixed-staggering patterns, introducing a novel approach to wind farm layout optimization. By employing the ADM with LES, this study provides insights into the combined effects of horizontal and vertical staggering on wake recovery, turbulence statistics, and power generation. In particular, vertically staggered layouts are shown to leverage vertical wind shear within the atmospheric boundary layer, enhancing downstream energy generation and mitigating wake interference. This study addresses the existing research gaps as well as offers practical guidance for improving wind farm design, contributing to more energy-efficient configurations that reduce power losses due to wake effects.

2. Modelling

2.1. Problem description

The configuration of wind turbines within a farm plays a critical role in optimizing power generation and understanding flow dynamics. In this study, we focus on evaluating different turbine layouts to analyze

their impact on flow dynamics, wake interactions, and power generation. By systematically studying aligned, horizontally staggered, vertically staggered, and mixed configurations, we aim to identify patterns that enhance flow recovery and maximize energy output. This work does not discuss the aerodynamic loading but rather emphasizes the flow behavior and energy extraction characteristics across these layouts.

Fig. 1 represents the different types of configurations considered in this study. Aligned layouts (Fig. 1a) serve as the baseline configuration in which turbines are placed uniformly in a grid pattern, maintaining equal spacing in both streamwise and spanwise directions. This simple arrangement, while efficient in design and construction, often results in

significant wake effects that reduce power generation efficiency for downstream turbines [46]. By providing a uniform reference case, the aligned layout allows for comparison with other, more complex patterns to highlight the benefits of staggered arrangements.

The horizontally staggered (Fig. 1b) configuration introduces a lateral offset between consecutive rows of turbines, shifting each row by a fraction of the spanwise spacing. This pattern helps mitigate the adverse effects of wake interactions by enhancing flow recovery and redistributing the wake field. The staggered rows create an alternating flow path that promotes higher energy availability for downstream turbines, thereby improving power generation efficiency relative to the

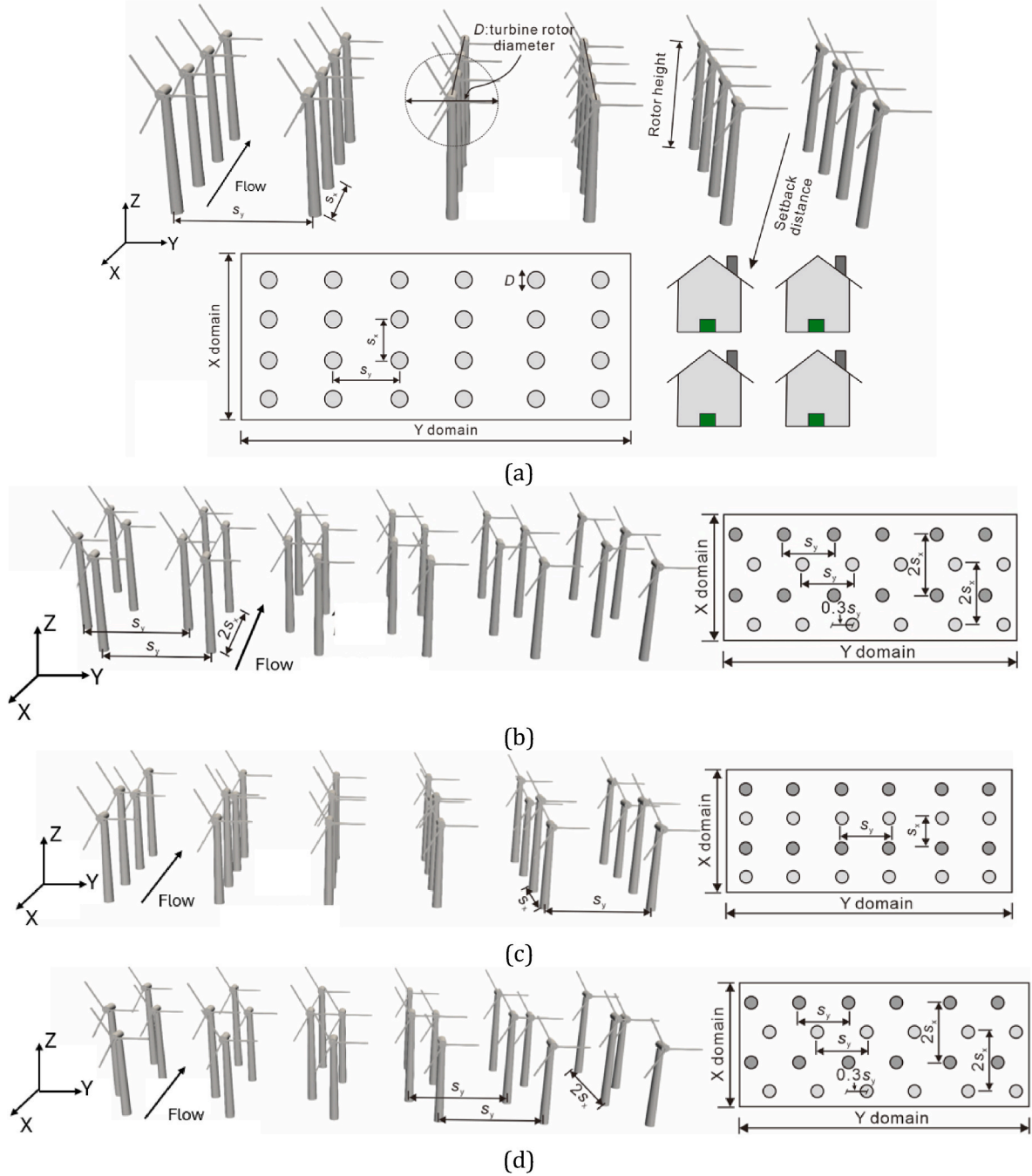


Fig. 1. Visualization of turbine layout configurations studied in this paper: (a) Aligned configuration with uniform spacing in both streamwise (S_x) and spanwise (S_y) directions, (b) Horizontally staggered configuration with a lateral offset of 30 % of spanwise spacing between consecutive rows, (c) Vertically staggered configuration with alternating turbine heights between rows, and (d) Mixed configuration combining horizontal staggering with vertical staggering by alternating turbine heights. The circles represent the location of the turbines while the dark circles indicate where the staggering is done. These figures are not properly scaled [48].

aligned configuration [52]. In this study, we have considered 10 %, 15 %, 30 % and 50 % horizontally staggered configurations.

In the vertically staggered (Fig. 1c) layout, turbines are alternated between two different heights across consecutive rows. This design creates vertical separation between the wakes, encouraging mixing and faster wake recovery. By disrupting the direct wake alignment typical of uniform-height rows, this configuration helps maintain a steadier flow and greater energy extraction for downstream turbines. In this study, we have considered a 25 % vertically staggered configuration.

The mixed configuration (Fig. 1d) combines both horizontal and vertical staggering to further enhance the advantages of these individual approaches. Rows are laterally offset while turbine heights alternate within each row, maximizing both lateral and vertical mixing of the wakes. This combination is designed to exploit the synergistic effects of wake redistribution and flow recovery, resulting in improved power generation efficiency. The mixed layout represents a more complex, yet potentially more effective, design for optimizing the performance of wind farms. In this study, we have considered the combination of 30 % horizontally and 25 % vertically staggered pattern as the mixed configuration.

By comparing the flow dynamics and power outputs of these configurations, this study provides valuable insights into how turbine placement can be optimized to achieve higher power generation and better wake management.

2.2. Governing equations

This investigation employs LES along with the Lagrangian scale-dependent dynamic approach [49] to model the turbulent atmospheric boundary layer. While comprehensive code documentation exists in earlier works [49–51], we focus our discussion on two key aspects: the atmospheric modeling framework (subsection 2.2.1) and the modeling of wind turbines (subsection 2.2.2).

2.2.1. Modeling atmospheric boundary layer

The computational analysis employs a LES code that computes the filtered, incompressible Navier-Stokes equations under neutral atmospheric conditions with pressure gradient forcing [53]:

$$\partial_t u_i = 0 \quad (1)$$

$$\partial_t u_i + u_j (\partial_j u_i - \partial_i u_j) = -\partial_i \left(\frac{p^*}{\rho} \right) + \partial_j \partial_j u_i + f_i - \partial_j \tau_{ij}^d - \partial_i \left(\frac{p_\infty}{\rho} \right) \delta_{i1} \quad (2)$$

The filtered velocity component is denoted by u_i , while p^* represents the modified pressure term, comprising the pressure p , kinetic energy ($1/2 \rho u_i u_i$), and the trace of the subgrid-scale stress tensor ($1/3 \tau_{kk}$). The deviatoric component of the subgrid-scale stress tensor (τ_{ij}^d) is computed using the Lagrangian scale-dependent dynamic framework [49], expressed as $\tau_{ij}^d = -2 (c_s \Delta)^2 |S| S_{ij}$, where c_s is evaluated through dual test-filtering operations. The flow is maintained by an imposed mean pressure gradient ($\frac{dp_\infty}{dx}$), and given the high Reynolds number conditions, viscous effects are considered negligible. The lower boundary implements an aerodynamic roughness length of $z_0 = 1 \times 10^{-4} H$, equivalent to 0.1 m. Wind turbine effects are incorporated through a drag force opposing the mean pressure-driven flow, represented in the force term f_i . The Einstein summation convention applies to repeated indices in Equations (1) and (2), with the pressure gradient forcing active only in the streamwise direction (x_1). For clarity, the coordinate system and velocity components are defined as: streamwise (x, u), spanwise (y, v), and wall-normal (z, w).

The computational domain features periodic boundary conditions in both streamwise (x) and spanwise (y) directions, enabling efficient simulation of extensive wind farm configurations. The domain extends 1000 m vertically (H) and approximately 3142 m in both horizontal directions (L). The numerical discretization employs $192 \times 192 \times 97$

grid points, with spatial resolutions of $\Delta x = \Delta y = 16.4$ m horizontally and $\Delta z = 10.4$ m vertically.

All LES simulations maintain consistent non-dimensional pressure gradient ($\frac{dp_\infty}{dx}$) and boundary layer height (H), though real atmospheric boundary layers would adjust their height based on wind farm roughness. The unconventional vertical forcing methodology alters the effective surface roughness, but this modification cannot be predicted theoretically. Given the computational constraints preventing dynamic domain height adjustment, the roughness changes affect the bulk flow velocity relative to the velocity scale $u_p = \sqrt{\frac{dp_\infty}{dx} \frac{H}{\rho}}$. To address this velocity variation, sometimes results, at the top of the domain, are normalized by the mean velocity (U). While an alternative approach would involve implementing a variable pressure gradient to maintain consistent mean velocity across simulations, the post-processing normalization method achieves equivalent results with greater simplicity.

2.2.2. Modeling wind turbines

The wind turbine modeling framework incorporates comprehensive configurations of domain parameters, model settings, boundary conditions, and turbine setups to accurately simulate flow dynamics and turbine interactions. As we have already mentioned before, the computational domain spans $3142 \text{ m} \times 3142 \text{ m} \times 1000 \text{ m}$, with grid resolutions of $192 \times 192 \times 97$, and non-uniform grid spacing ($\Delta x = \Delta y = 16.4 \text{ m}$, $\Delta z = 10.4 \text{ m}$). A Lagrangian Scale-Dependent Subgrid-Scale (SGS) model is employed to capture turbulence dynamics, complemented by a cut-off filter. Coriolis forcing is excluded for this setup but is intended for future location-specific simulations. Boundary conditions include an equilibrium wall model for the lower boundary and stress-free conditions for the upper boundary. Averaging is applied in the x - y plane, and the simulation runs for longer durations for capturing fully developed turbulence. The simulations are performed using LESGO code which is an open-source code developed by Johns Hopkins University and publicly available at <https://lesgo.me.jhu.edu/>.

The turbine setup consists of a 4×6 array of turbines, each with a rotor diameter and height of 100 m. All computational details are listed in Table 1. Since we are imposing periodic boundary conditions in streamwise and spanwise directions, this array can represent a full wind farm. We have only considered the onshore wind farm setup in this study. It is already mentioned that we have employed Actuator Disk Model (ADM) to simulate the whole wind farm. The ADM approximates the turbine as a disk that extracts kinetic energy from the wind. While this approach effectively captures the primary wake effects, incorporating multiple turbine models with varying rotor diameters, hub heights, and thrust coefficients could further improve the generalizability and accuracy of wake predictions. The turbines are placed uniformly in both spanwise and streamwise directions, although the distances between them in each direction differ. Due to periodicity, the spanwise spacing of the wind turbine is $S_y = \frac{L_y}{N_{sp}}$ where L_y is the spanwise length and N_{sp} is the number of turbines in the spanwise direction.

Table 1
Computational details of the simulations.

Cases	$L_x(\text{km}) \times L_y(\text{km}) \times H(\text{km})$	$N_x \times N_y \times N_z$	$N_{st} \times N_{sp}$	Positioning and % of staggering
A1	$\pi \times \pi \times 1$	$128 \times 128 \times 128$	4×6	0 % (Aligned)
A2	$\pi \times \pi \times 1$	$192 \times 192 \times 97$	4×6	0 % (Aligned)
H1	$\pi \times \pi \times 1$	$192 \times 192 \times 97$	4×6	10 %, 15 %, 30 %, 50 % (Horizontal)
V1	$\pi \times \pi \times 1$	$192 \times 192 \times 97$	4×6	25 % (Vertical)
M1	$\pi \times \pi \times 1$	$192 \times 192 \times 97$	4×6	30 % Horizontal & 25 % Vertical (Mixed)

Similarly, the streamwise spacing of the wind turbine is $S_x = \frac{L_x}{N_{st}}$ where L_x is the streamwise length and N_{st} is the number of turbines in the streamwise direction. When the effects of alignment is studied, the layout of the wind farm is adjusted by the % of offset which corresponds to angle $\psi = \arctan\left(\frac{S_{dy}}{S_x}\right)$ where S_{dy} is the spanwise offset of turbine row to the next [52]. For the aligned setup, the value of ψ is 0. The variation of ψ is done in such a way that the number of turbines remains fixed. It should be noted that this study will not provide an optimal layout in general since real-world wind farms depend on annual wind distribution at that specific location. Different configurations, including aligned, vertically staggered, horizontally staggered and a combination of horizontal and vertical (mixed) staggered layouts, are analyzed to assess the impact of turbine layout on wake interactions and power generation. These configurations provide insights into optimizing turbine placements to minimize wake losses. This framework establishes a robust foundation for investigating turbine array performance and developing strategies for enhanced wind energy generation.

• Thrust Force Modeling via Actuator Disk Theory

To optimize computational efficiency and avoid requirements for high spatiotemporal resolution, wind turbines are simulated using the actuator disk methodology [54,55]. This approach represents each turbine's flow interaction through a distributed thrust force formulation, defined as:

$$F_x = -\frac{1}{2}C_T\rho(u_d^T)^2 A_T \quad (3)$$

The term C_T represents the modified thrust coefficient (referenced to

the disk velocity rather than the upstream velocity, as detailed in Ref. [50]). In the Betz limit, the value of C_T is 2. In this present study, a constant value of 1.33 is used for C_T [50]. The variable u_d^T denotes the disk-averaged velocity, which undergoes temporal smoothing via a first-order exponential filter with a characteristic timescale. A_T represents the total swept area of the rotor. The simulation incorporates 24 wind turbines, each with a diameter (D) and hub height (z_h) of $0.1H$, equivalent to 100 m. The thrust force is spatially distributed using a Gaussian-filtered indicator function, ensuring smooth variation to maintain numerical stability in the pseudo-spectral derivative calculations. The instantaneous power extraction for each turbine is calculated as the product of the applied drag force and the time-filtered disk-averaged velocity:

$$P = F_x u_d^T = -\frac{1}{2}C_T\rho(u_d^T)^3 A_T \quad (4)$$

Further comprehensive documentation regarding the actuator disk model implementation methodology can be found in previous studies [50–52].

3. Results and discussions

3.1. Grid resolution study

The grid resolution study was conducted to evaluate the sensitivity of the results in large-eddy simulations (LES). Two grid resolutions, $128 \times 128 \times 128$ (coarser grid) and $192 \times 192 \times 97$ (finer grid) were compared to assess their ability to capture key turbulence statistics. These grid resolutions were already used in the previous literature for similar domain length [48,53]. This study is critical for ensuring that the

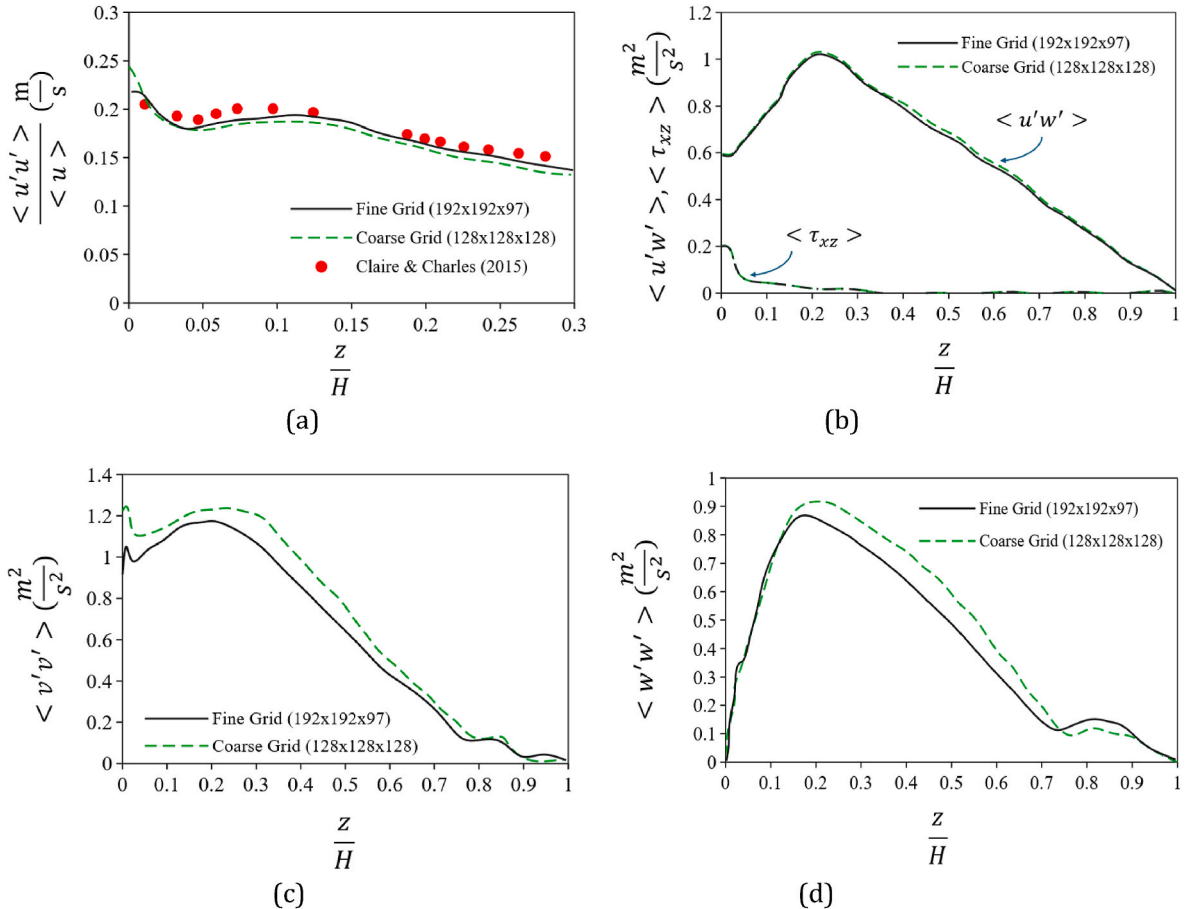


Fig. 2. Effect of grid resolution on different turbulent statistics.

selected grid resolution can accurately capture the complex interactions between atmospheric turbulence and turbine wakes, which are essential for optimizing wind farm performance.

Fig. 2 demonstrates significant differences between the two grid resolutions in their ability to resolve turbulence intensities. The finer grid ($192 \times 192 \times 97$) provided higher accuracy, resolving the smaller scale eddies. For example, the streamwise velocity variance ($\langle u'u' \rangle / \langle u \rangle$) from the finer grid closely matched the simulation results of Claire & Charles [53]. Similarly, the finer grid better resolved the turbulent intensities like $\langle w'w' \rangle$ and $\langle u'w' \rangle$. In contrast, the coarser grid overestimated turbulence intensities, demonstrating limitations in resolving small-scale turbulent structures. Fig. 3 shows the 3D contours of streamwise velocity in the wind farm simulation at coarser and finer grid resolution. The z locations are chosen in such a way that they show the changes in the turbulence structures very clearly. $z/H = 0, 0.05, 0.1$, and 0.15 show the turbulent structures near the ground, at the center of the rotor, at the top of the turbine and far from the turbine. It is also evident from the figure that at low resolution the small-scale turbulence is not well resolved and there is the existence of large-scale structures.

These findings underscore the importance of grid resolution in LES simulations on wind farm performance and wake interactions. The finer grid resolution provides both improved fidelity in turbulence modeling and ensures better alignment with previous observations. The ability to resolve small scale turbulence and momentum transport accurately is critical for understanding turbine wake recovery and optimizing wind farm layouts.

3.2. Power improvement in horizontally staggered patterns

Horizontal staggering of turbines in wind farms significantly influences wake dynamics, energy extraction, and overall farm performance. By varying the horizontal offset between turbine rows, it is possible to manipulate the wake interaction and enhance downstream flow recovery, thereby optimizing the power generation [27,28,45]. In this study, we systematically analyzed horizontal staggered configurations with offsets of 10 %, 15 %, 30 %, and 50 % relative to the turbine spacing. These configurations are explored to identify the impact of varying degrees of staggering on power production and wake mitigation. The selected staggered patterns represent a spectrum of offsets commonly considered in wind farm design, allowing a comprehensive assessment of their operational implications.

Fig. 4 represents the streamwise velocity distribution at multiple vertical positions (z/H) for three distinct wind turbine layouts: aligned,

30 % horizontal staggered, and 50 % horizontal staggered configurations. The higher values of streamwise velocity indicate the faster flow and lower values indicate the regions with wake effects or turbulence. The main goal of this analysis is to assess the impact of staggered configurations on wake development, flow dynamics and power generation.

In the aligned layout, the turbines are positioned directly downstream of one another (Fig. 4a). This results in highly structured wake patterns, as evidenced by distinct regions of reduced velocity downstream of each turbine. The wake recovery is slower due to the alignment of the turbines, leading to pronounced velocity deficits at multiple heights (z/H). At lower heights ($z/H < 0.05$), the velocity reduction is most significant, indicating strong wake interactions. This configuration demonstrates the highest degree of wake overlap, contributing to lower overall power generation [31,32]. In the 30 % horizontal staggered configuration, the turbines are shifted laterally by 30 % of their spacing. This layout disrupts the direct wake alignment observed in the fully aligned case, resulting in improved wake mixing and faster velocity recovery at downstream locations. The velocity contours exhibit a more diffused pattern compared to the aligned configuration, especially at mid-level heights ($z/H = 0.05$). This staggered layout reduces the wake interaction between successive turbines, leading to better flow dynamics and more energy-efficient performance in downstream turbines. The 50 % horizontal staggered layout further increases the lateral offset between turbines, creating the most dispersed wake patterns among the three configurations. The velocity contours reveal improved wake recovery, particularly at higher levels ($z/H = 0.1$). The wake effects are less concentrated and exhibit greater mixing with the surrounding flow [45].

After we understand the behavior of streamwise velocity at different heights of the domain, we want to explore the behavior of mean velocity at different staggered patterns. Fig. 5 shows the variation of normalized mean velocity with height of the domain at different staggered patterns. This mean velocity profiles provide an insight into wake recovery dynamics. The aligned configuration exhibits the slowest velocity recovery at the turbine regions ($z/H < 0.1$). The persistent wake interference limits energy distribution into the flow, resulting in lower mean velocities. The 30 % staggered layout achieves the fastest velocity recovery in the turbine region. The increased lateral spacing promotes turbulence mixing and momentum transfer, leading to higher velocity recovery downstream.

Fig. 6 shows the average power output at different staggered patterns. For a better understanding of the comparison, only aligned, 30 %, and 50 % horizontally staggered patterns are shown in Fig. 6a. The

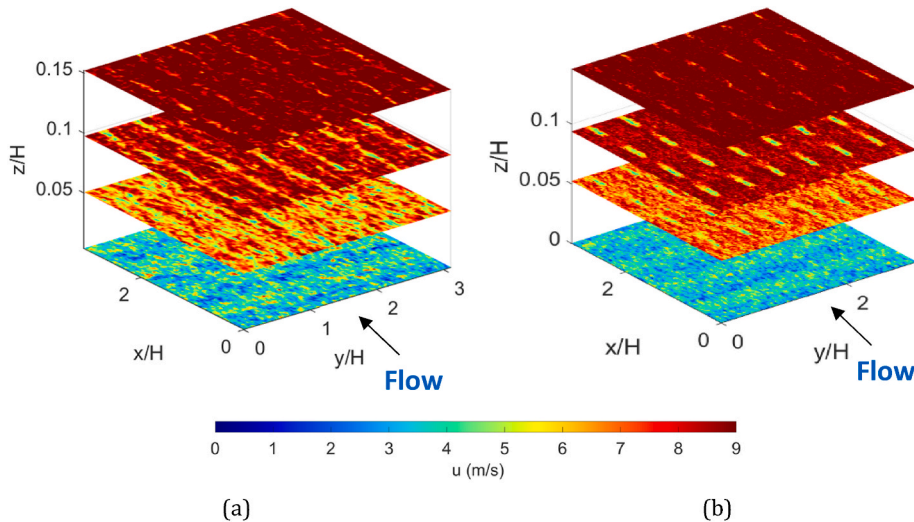


Fig. 3. 3D contours of streamwise velocity in the wind farm simulation at grid resolution (a) $128 \times 128 \times 128$ (b) $192 \times 192 \times 97$. At low resolution the small-scale turbulence is not well resolved, and large-scale structures are evident in the figure.

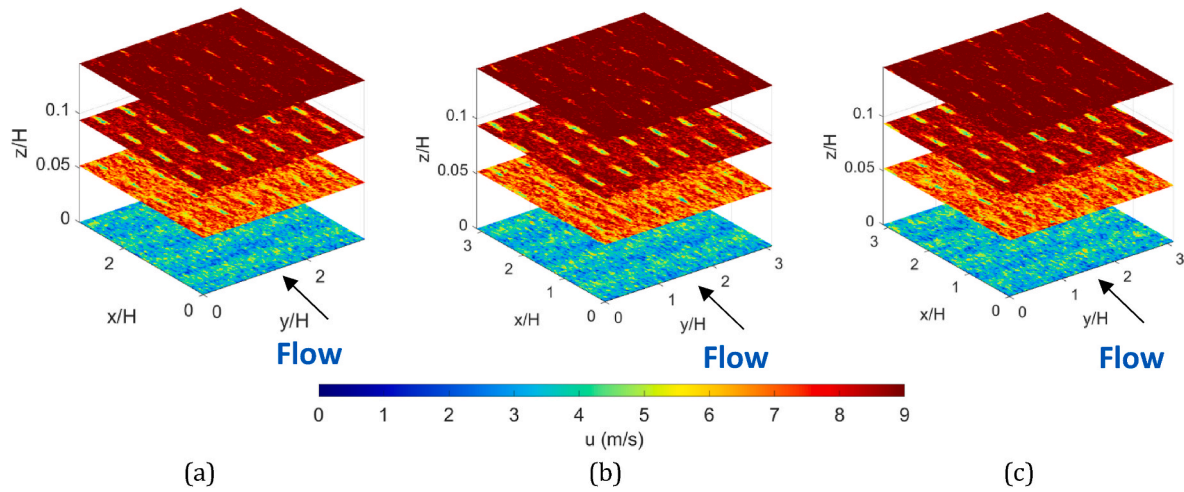


Fig. 4. 3D contours of streamwise velocity in the wind farm simulation at (a) aligned (b) 30 % horizontally staggered (c) 50 % horizontally staggered patterns. The z locations are chosen in such a way that it shows the changes in the turbulence structures very clearly. $z/H = 0, 0.05, 0.1$ and 0.14 show the turbulent structures near the ground, at the center of the rotor, at the top of the turbine and far from the turbine.

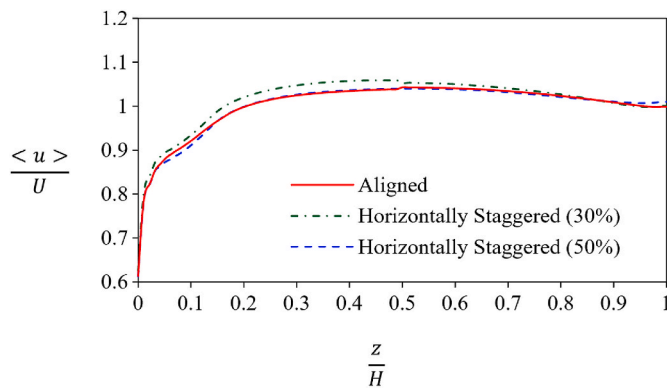


Fig. 5. The mean velocity profiles at different horizontally staggered patterns.

corresponding values of alignment angle ψ for aligned, 30 %, and 50 % horizontally staggered patterns are 0° , 11.304° and 18.42° respectively. The aligned configuration experiences the most rapid decline in power output after the initial peak. The lack of lateral staggering results in severe wake interactions, leading to significant energy deficits. This aligns with the earlier wake structure analysis, where the aligned layout

exhibited slow wake recovery and high velocity deficits [31,32]. The 30 % staggered configuration shows improved performance compared to the aligned layout. The partial staggering mitigates wake interference, enhancing turbulence mixing and wake recovery, which results in higher power generation. While the 50 % staggered layout still performs better than the aligned configuration, its performance is slightly lower than the 30 % staggered case. This results from increased turbulence diffusion at higher staggering levels, which reduces the localized velocity gradients available for downstream turbines [45].

Contrary to what might be expected, the 30 % staggered layout achieves the highest average power output outperforming both the aligned and all the staggered configurations (Fig. 6b). The phenomenon of achieving maximum power output at an intermediate alignment angle, rather than a fully staggered configuration, can be attributed to the interplay between wake recovery dynamics and wake interference. At intermediate angles, the turbine layout facilitates enhanced wake recovery by promoting increased vertical and horizontal kinetic energy mixing. This reduces energy deficits to the downstream turbines while maintaining beneficial wake interactions. In fully staggered layouts, although wake overlap is minimized, the turbines are separated too much leading to less efficient energy recovery. Hence, the intermediate staggered layout strikes an optimal balance, leading to better overall power generation. This observation aligns with the findings of Stevens

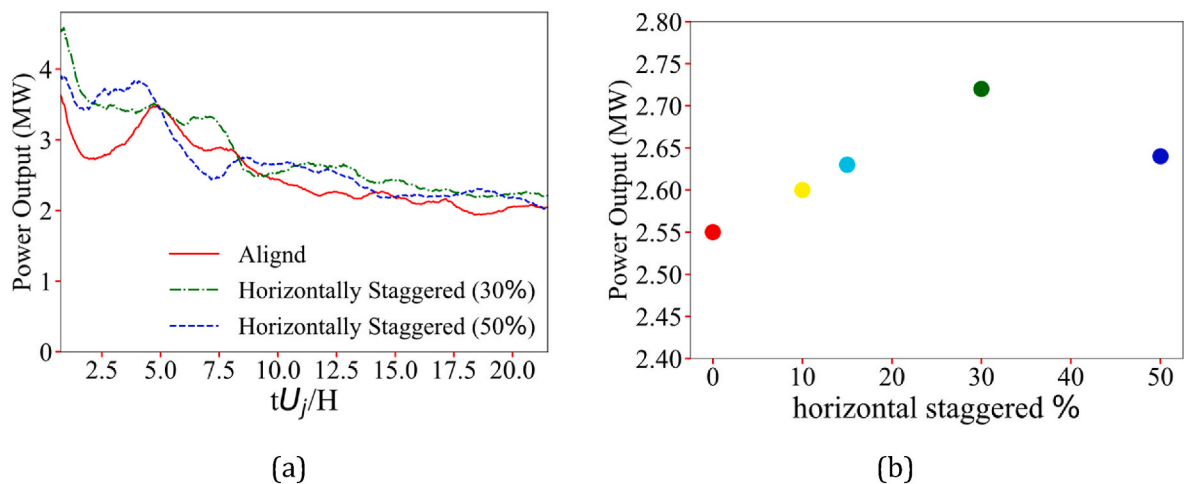


Fig. 6. The average power output at different staggered patterns.

et al. [52] who reported that the highest power generation occurs at an intermediate alignment angle of approximately 11° . They found that at an intermediate angle, first several rows of turbines fall outside wakes of the upstream turbine rows leading to highest average power generation. In our study, the 30 % staggered layout corresponds to an alignment angle of approximately 11.304° , yielding similar performance. These results underscore the importance of optimizing turbine alignment to keep a balance between minimizing wake interference and maximizing kinetic energy recovery, leading to the improvement of overall wind farm performance.

3.3. Power improvement in vertically staggered patterns

In the previous section, we discussed the effects of horizontal staggering on the flow dynamics and power generation of the wind farm. In this section, we want to extend our analysis to investigate the effects of vertical staggering on the power generation of wind farms. The vertical staggering has rarely been reported in the literature and that is why we are interested in investigating its effect on power generation [35]. In this study, we have considered a 25 % vertically staggered pattern and compared it with the aligned cases to show the improvement of power output. We have not considered a higher percentage of vertical staggering since it might cause the stability issue of the wind turbine which is the scope of study for our next paper.

Fig. 7 demonstrates the impact of vertically staggered patterns on the streamwise velocity at multiple heights (z/H). As we have already discussed, in the aligned pattern, the turbines are positioned without any vertical offset. The wakes from upstream turbines are clearly visible as regions of reduced velocity extending downstream. These regions exhibit slow recovery due to the strong wake interference from consecutive turbines. At lower heights ($z/H \leq 0.05$), the wakes are more concentrated, indicating reduced mixing and minimal distribution of energy in the flow. This results in significant velocity deficits that exist in downstream locations. The aligned configuration shows highly structured wake patterns and poor flow recovery, which aligns with earlier findings [31,32]. The 25 % vertical staggered layout introduces vertical offsets between consecutive turbines, resulting in more dispersed wake patterns. The staggered layout breaks the alignment of wake structures, promoting greater turbulence mixing. The velocity contours show a more distributed wake pattern, especially at mid heights ($z/H \sim 0.05$). At

all heights, the wake regions exhibit faster velocity recovery compared to the aligned layout. This is particularly evident at higher levels ($z/H = 0.1$), where the wakes are less pronounced, and energy distribution occurs more efficiently. The staggered configuration reduces the direct wake overlap, resulting in a more uniform distribution of velocity across the downstream region. This uniformity suggests better downstream energy availability for subsequent turbines.

Fig. 8 shows the average power output in vertical staggering compared to the aligned pattern. The 25 % vertically staggered configuration consistently delivers higher power output, attributed to reduced wake interference and improved turbulence mixing from vertical offsets between turbines [35]. This layout exploits the vertical wind shear within the ABL and provides higher power output. This layout also disrupts wake alignment, enabling flow interaction, and promoting faster wake recovery. Overall, the vertical staggering proves to be an effective strategy for enhancing power generation without increasing turbine spacing.

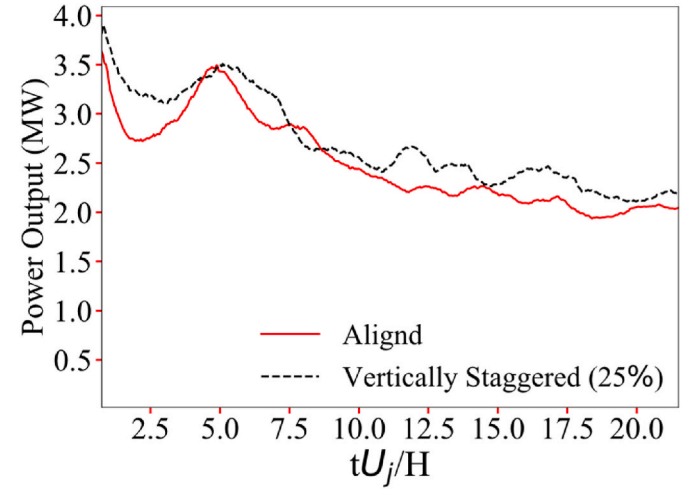


Fig. 8. Average power output in 25 % vertically staggered pattern in terms of aligned pattern. It is evident that the vertical staggering gives higher average power output than aligned pattern.

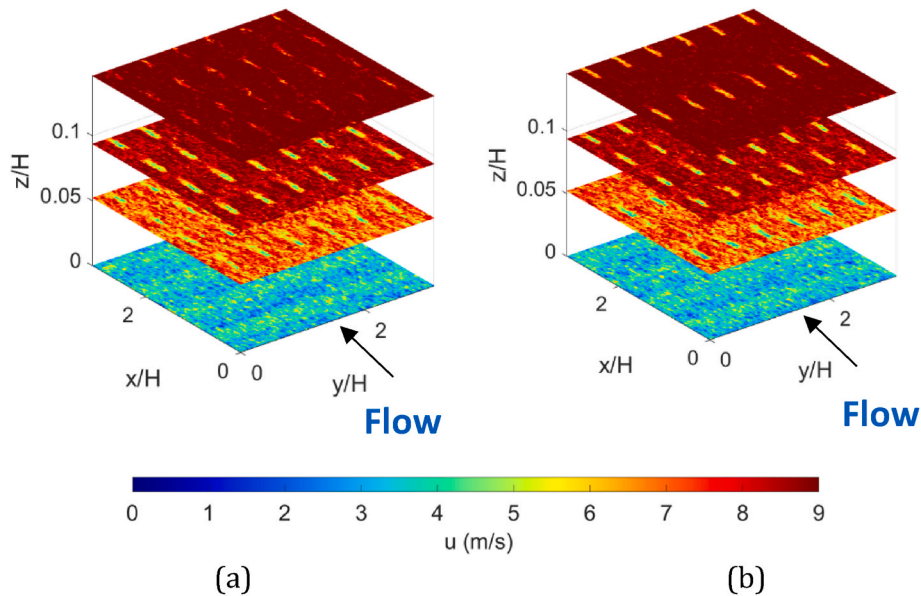


Fig. 7. 3D contours of streamwise velocity in the wind farm simulation at (a) aligned (b) 25 % vertically staggered patterns. The z locations are chosen in such a way that it shows the changes in the flow structures very clearly. $z/H = 0, 0.05, 0.05$ and 0.15 show the turbulent structures near the ground, at the center of the rotor, near the top of the turbine and far from the turbine.

3.4. Power improvement in mixed (horizontal & vertical) staggered patterns

In the earlier sections, we investigated the effects of horizontal and vertical staggering on wake recovery, flow dynamics, and power generation in wind farm simulations. Our findings showed that both horizontal and vertical staggering improve average power output compared to the aligned configuration. Based on these promising results, this section focuses on combining the two strategies to maximize power generation. Specifically, since 30 % horizontal staggering produced the highest power output, we combined it with 25 % vertical staggering to investigate the effects of this mixed staggered pattern.

The mixed staggered configuration, which combines horizontal (30 %) and vertical (25 %) staggering, exhibits remarkable improvements in flow dynamics and power output compared to aligned, purely horizontal, and purely vertical staggered layouts. The mean velocity profile demonstrates that the mixed configuration achieves the fastest velocity recovery, surpassing all other configurations (Fig. 9). This enhanced wake recovery from the lateral and vertical offsets disrupts the wake structure more effectively. The staggered layout ensures greater turbulence mixing and facilitates energy distribution into wake regions.

The power output trends further validate the advantages of the mixed staggered approach. Initially, all configurations show similar peak power output due to the undisturbed inflow conditions. However, as wakes develop and interact downstream, the mixed staggered configuration consistently maintains the highest power output over time (Fig. 10a). This higher average power generation is due to the combined benefits of horizontal and vertical staggering, which minimize wake overlap, promote faster wake recovery, and enhance energy availability for the downstream turbines. Compared to the aligned configuration, the mixed layout demonstrates significant mitigation of power losses, while outperforming the purely horizontally and vertically staggered layouts. These results tell us about the potential of mixed staggered configurations to optimize wind farm performance, particularly in scenarios of space constraints. The combined approach maximizes the average power outcome while ensuring a more stable and robust power generation process.

Another interesting observation from Fig. 10 is that the horizontal staggering is more effective than the vertical staggering in terms of power generation. The reason is that it reduces direct wake overlap, allowing downstream turbines to capture higher wind speeds while promoting faster wake recovery through horizontal mixing of kinetic energy. Unlike vertical staggering, which relies on vertical wind shear and is sensitive to atmospheric conditions, horizontal staggering provides more consistent performance [29,52].

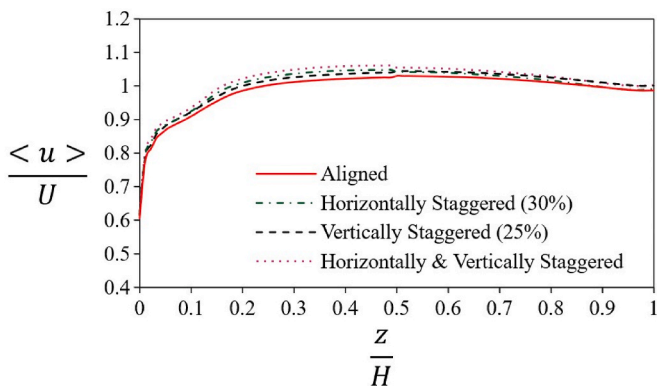


Fig. 9. The mean velocity profiles at aligned, purely horizontal, purely vertical and mixed staggered patterns.

4. Concluding remarks

This study investigates the effects of turbine layout configurations on flow dynamics, wake recovery, and power output in large wind farms. Using robust and highly accurate large-eddy simulations (LES), we evaluated the performance of aligned, horizontally staggered, vertically staggered, and mixed horizontal-vertical staggered layouts. To establish the numerical accuracy, we performed a very rigorous grid resolution study, and the findings offer a robust framework for optimizing wind farm performance in the onshore wind farm settings.

A grid resolution study was conducted as a foundational step to ensure the accuracy and reliability of the LES simulations. Two resolutions, $128 \times 128 \times 128$ and $192 \times 192 \times 97$, were compared and found that the finer grid better captured the turbulence statistics and resolved the small-scale turbulence. This study demonstrates the necessity of high-resolution simulation for accurately resolving the complex flow structures and wake interactions in wind farm simulations.

For purely horizontal staggering, the 30% staggered configuration demonstrated significant improvements over the aligned and other staggered layouts. By introducing lateral offsets, horizontal staggering disrupted wake alignment and enhanced wake mixing, resulting in faster velocity recovery and consistently higher power output. The power output trends clearly showed that horizontal staggering reduces wake interference observed in the aligned layout, offering a practical solution for improving overall power generation in wind farms.

For the vertically staggered configuration, the height benefit reduces wake overlap. Vertical staggering allows downstream wakes to interact with higher-momentum flow, promoting better wake recovery and more uniform energy distribution across the farm. Compared to the aligned layout, vertical staggering showed better performance in both wake recovery and power output.

The mixed configuration, combining 30 % horizontal and 25 % vertical staggering, has been found to be the optimum configuration. This arrangement used the benefits of both lateral and vertical staggering, achieving the fastest wake recovery and highest power output among all configurations. By disrupting wake interactions, the mixed configuration maximized turbulence mixing and energy distribution, ensuring robust and maximum power generation. These findings highlight the potential of multi-dimensional staggering for optimizing wind farm performance.

Beyond improving energy output, optimizing wind farm layouts can significantly reduce operational costs, making wind energy more economically competitive. Enhanced wake recovery reduces the need for excess turbines, lowering capital expenditure, while improved power generation increases revenue per turbine, enhancing long-term profitability. It is very important to consider both power generation and financial viability while designing the wind farms, ensuring that the optimized layouts are more productive and cost-effective in real-world applications.

Overall, this study highlights the critical role of turbine layout in mitigating wake interference and enhancing wind farm power generation. The results demonstrate that while horizontal and vertical staggering independently provide significant power enhancement, their combined implementation through mixed staggering offers the most effective solution. Future research could explore the integration of these layouts with dynamic control strategies, atmospheric stratification effects, and offshore conditions to further enhance wind energy sustainability and scalability.

While this study demonstrates significant potential, several aspects remain unexplored and will be addressed in future research. A more practical approach would involve studying finite-size wind farms using both LES and analytical models to bridge the gap between theory and real-world applications. It is important to note that this work does not aim to determine the universally optimal wind farm layout, as such a determination depends on numerous factors, including site-specific conditions and annual wind distributions, which are beyond the scope

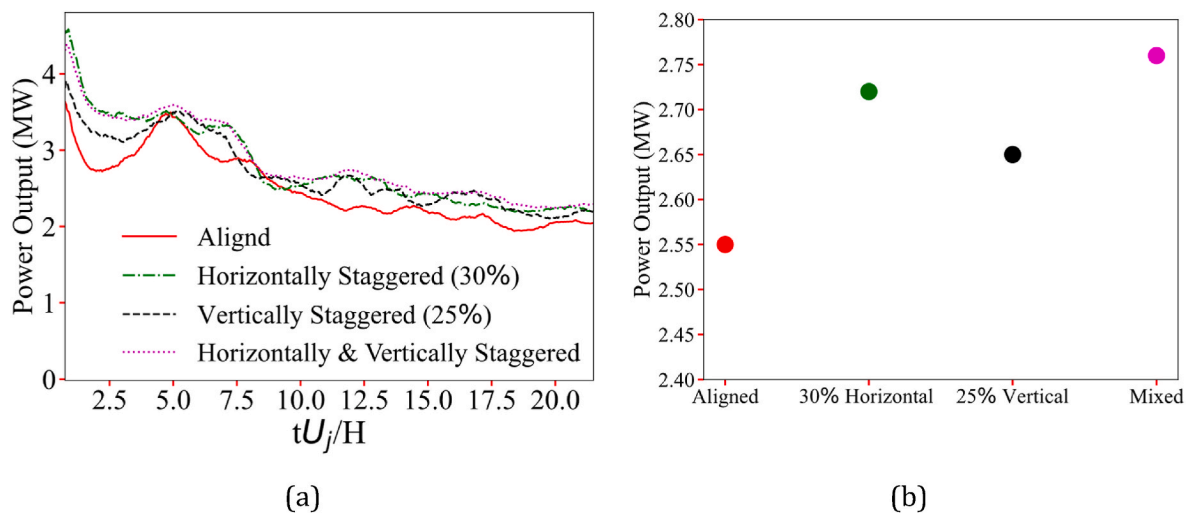


Fig. 10. (a) The average power output over time for aligned, purely horizontal, purely vertical and mixed patterns. (b) Higher power output for mixed pattern compared to purely horizontal and purely vertical patterns.

of this study. Furthermore, incorporating multiple turbine models with varying rotor diameters, hub heights, and thrust coefficients would provide deeper insights into how turbine design influences wake recovery and power generation. In future work, we plan to address these challenges and conduct more comprehensive and robust analyses.

CRediT authorship contribution statement

Muhammad Rubayat Bin Shahadat: Writing – review & editing, Writing – original draft, Validation, Software, Methodology, Investigation, Formal analysis, Conceptualization. **Mohammad Hossein Doranehgard:** Writing – review & editing, Writing – original draft, Conceptualization, Data curation, Formal analysis, Investigation, Validation, Visualization. **Weibing Cai:** Visualization, Software. **Zheng Li:** Writing – review & editing, Writing – original draft, Supervision, Resources, Project administration, Methodology, Investigation, Funding acquisition, Formal analysis, Conceptualization.

Declaration of competing interest

The authors declare that they have no known competing financial interests or personal relationships that could have appeared to influence the work reported in this paper.

Acknowledgements

Professor Charles Meneveau (meneveau@jhu.edu) and Professor Benjamin Schafer (schafer@jhu.edu) from Johns Hopkins University are well acknowledged for initial discussions about the topic, as well as in helping with implementing and running the LES tool: LESGO code which is an open-source code developed by Johns Hopkins University and publicly available at <https://lesgo.me.jhu.edu/>.

This material is based upon work supported by the U.S. Department of Energy's Office of Energy Efficiency and Renewable Energy (EERE) under the Wind Energy Technologies Office (WETO) Award Number DE-EE0011269.

This report was prepared as an account of work sponsored by an agency of the United States Government. Neither the United States Government nor any agency thereof, nor any of their employees, makes any warranty, express or implied, or assumes any legal liability or responsibility for the accuracy, completeness, or usefulness of any information, apparatus, product, or process disclosed, or represents that its use would not infringe privately owned rights. Reference herein to any specific commercial product, process, or service by trade name,

trademark, manufacturer, or otherwise does not necessarily constitute or imply its endorsement, recommendation, or favoring by the United States Government or any agency thereof. The views and opinions of authors expressed herein do not necessarily state or reflect those of the United States Government or any agency thereof.

Abridged Legal Disclaimer: "The views expressed herein do not necessarily represent the views of the U.S. Department of Energy or the United States Government."

Data availability

Data will be made available on request.

References

- [1] Mushtaq K, Waris A, Zou R, Shafique U, Khan NB, Khan MI, et al. A comprehensive approach to wind turbine power curve modeling: addressing outliers and enhancing accuracy. *Energy* 2024;304:131981. <https://doi.org/10.1016/j.energy.2024.131981>.
- [2] Cheng B, Yao Y, Qu X, Zhou Z, Wei J, Liang E, et al. Multi-objective parameter optimization of large-scale offshore wind Turbine's tower based on data-driven model with deep learning and machine learning methods. *Energy* 2024;305:132257. <https://doi.org/10.1016/j.energy.2024.132257>.
- [3] Vargas SA, Esteves GRT, Maçaira PM, Bastos BQ, Cyrino Oliveira FL, Souza RC. Wind power generation: a review and a research agenda. *J Clean Prod* 2019;218:850–70. <https://doi.org/10.1016/j.jclepro.2019.02.015>.
- [4] Gielen D, Boshell F, Saygin D, Bazilian MD, Wagner N, Gorini R. The role of renewable energy in the global energy transformation. *Energy Strategy Rev* 2019;24:38–50.
- [5] Liu J, Cai C, Song D, Zhong X, Shi K, Chen Y, et al. Nonlinear model predictive control for maximum wind energy extraction of semi-submersible floating offshore wind turbine based on simplified dynamics model. *Energy* 2024;311:133356. <https://doi.org/10.1016/j.energy.2024.133356>.
- [6] Liu Y, Zhao Z, Liu Y, Liu H, Wei S, Ma Y, et al. Combined wake control of aligned wind turbines for power optimization based on a 3D wake model considering secondary wake steering. *Energy* 2024;308:132900. <https://doi.org/10.1016/j.energy.2024.132900>.
- [7] Holttinen H, Groom A, Kennedy E, Woodfin D, Barroso L, Orths A, et al. Variable renewable energy integration: status around the world. *IEEE Power Energy Mag* 2021;19:86–96. <https://doi.org/10.1109/MPE.2021.3104156>.
- [8] Adhikari J, Prasanna IV, Panda SK. Power conversion system for high altitude wind power generation with medium voltage AC transmission. *Renew Energy* 2016;93:562–78. <https://doi.org/10.1016/j.renene.2016.03.004>.
- [9] He X, He B, Qin T, Lin C, Yang J. Ultra-short-term wind power forecasting based on a dual-channel deep learning model with improved coot optimization algorithm. *Energy* 2024;305:132320. <https://doi.org/10.1016/j.energy.2024.132320>.
- [10] Dou B, Qu T, Lei L, Zeng P. Optimization of wind turbine yaw angles in a wind farm using a three-dimensional yawed wake model. *Energy* 2020;209:118415. <https://doi.org/10.1016/j.energy.2020.118415>.
- [11] Ye M, Chen H-C, Koop A. High-fidelity CFD simulations for the wake characteristics of the NTNU BT1 wind turbine. *Energy* 2023;265:126285. <https://doi.org/10.1016/j.energy.2022.126285>.

- [12] Sun C, Tian T, Zhu X, Hua O, Du Z. Investigation of the near wake of a horizontal-axis wind turbine model by dynamic mode decomposition. *Energy* 2021;227:120418. <https://doi.org/10.1016/j.energy.2021.120418>.
- [13] Peng HY, Liu HJ, Yang JH. A review on the wake aerodynamics of H-rotor vertical axis wind turbines. *Energy* 2021;232:121003. <https://doi.org/10.1016/j.energy.2021.121003>.
- [14] Sande B, Van Der Pijl SP, Koren B. Review of computational fluid dynamics for wind turbine wake aerodynamics. *Wind Energy* 2011;14:799–819. <https://doi.org/10.1002/we.458>.
- [15] Sadeghian O, Oshnoei A, Tarafdar-Hagh M, Khezri R. A clustering-based techno-economic analysis for wind farm and shunt capacitor allocation in radial distribution systems. *Int Trans Electr Energy Syst* 2021;31. <https://doi.org/10.1002/2050-7038.12708>.
- [16] Ma K, Zhang H, Gao X, Wang X, Nian H, Fan W. Research on evaluation method of wind farm wake energy efficiency loss based on SCADA data analysis. *Sustainability* 2024;16:1813. <https://doi.org/10.3390/su16051813>.
- [17] Ali A, Abbas G, Keerio MU, Touti E, Ahmed Z, Alsalmán O, et al. A Bi-level techno-economic optimal reactive power dispatch considering wind and solar power integration. *IEEE Access* 2023;11:62799–819. <https://doi.org/10.1109/ACCESS.2023.3286930>.
- [18] Abbas G, Ali B, Chandni K, Koondhar MA, Chandio S, Mirsaedi S. A parametric approach to compare the wind potential of sanghar and gwadar wind sites. *IEEE Access* 2022;10:110889–904. <https://doi.org/10.1109/ACCESS.2022.3215261>.
- [19] Ali A, Aslam S, Mirsaedi S, Mugheri NH, Memon RH, Abbas G, et al. Multi-objective multiperiod stable environmental economic power dispatch considering probabilistic wind and solar PV generation. *IET Renew Power Gener* 2024;18:3903–22. <https://doi.org/10.1049/rpg2.13077>.
- [20] Ali B, Abbas G, Memon A, Mirsaedi S, Koondhar MA, Chandio S, et al. A comparative study to analyze wind potential of different wind corridors. *Energy Rep* 2023;9:1157–70. <https://doi.org/10.1016/j.egyr.2022.12.048>.
- [21] Abdollahi A, Ghadimi A, Miveh M, Mohammadi F, Jurado F. Optimal power flow incorporating FACTS devices and stochastic wind power generation using krill herd algorithm. *Electronics* 2020;9:1043. <https://doi.org/10.3390/electronics9061043>.
- [22] Bhurt F, Ali A, Keerio MU, Abbas G, Ahmed Z, Mugheri NH, et al. Stochastic multi-objective optimal reactive power dispatch with the integration of wind and solar generation. *Energies* 2023;16:4896. <https://doi.org/10.3390/en16134896>.
- [23] Porté-Agel F, Wu Y-T, Lu H, Conzemius RJ. Large-eddy simulation of atmospheric boundary layer flow through wind turbines and wind farms. *J Wind Eng Ind Aerod* 2011;99:154–68. <https://doi.org/10.1016/j.jweia.2011.01.011>.
- [24] Lanzilao L, Meyers J. A parametric large-eddy simulation study of wind-farm blockage and gravity waves in conventionally neutral boundary layers. *J Fluid Mech* 2024;979:A54. <https://doi.org/10.1017/jfm.2023.1088>.
- [25] Calaf M, Meneveau C, Meyers J. Large eddy simulation study of fully developed wind-turbine array boundary layers. *Phys Fluids* 2010;22:015110. <https://doi.org/10.1063/1.3291077>.
- [26] Burlando M, Ricci A, Freda A, Repetto MP. Numerical and experimental methods to investigate the behaviour of vertical-axis wind turbines with staters. *J Wind Eng Ind Aerod* 2015;144:125–33. <https://doi.org/10.1016/j.jweia.2015.04.006>.
- [27] Chamorro LP, Porté-Agel F. Turbulent flow inside and above a wind farm: a wind-tunnel study. *Energies* 2011;4:1916–36. <https://doi.org/10.3390/en4111916>.
- [28] Sickler M, Ummels B, Zaaijer M, Schmehl R, Dykes K. Offshore wind farm optimisation: a comparison of performance between regular and irregular wind turbine layouts. *Wind Energy Sci* 2023;8:1225–33. <https://doi.org/10.5194/wes-8-1225-2023>.
- [29] Markfort CD, Zhang W, Porté-Agel F. Turbulent flow and scalar transport through and over aligned and staggered wind farms. *J Turbul* 2012;13:N33. <https://doi.org/10.1080/14685248.2012.709635>.
- [30] Thiébot J, Guillou N, Guillou S, Good A, Lewis M. Wake field study of tidal turbines under realistic flow conditions. *Renew Energy* 2020;151:1196–208. <https://doi.org/10.1016/j.renene.2019.11.129>.
- [31] Zhang Y, Ji R, Sun K, Zhang Z, Zheng Y, Zhang J, et al. Research on complex wake interference of aligned rotors considering the precone variation of the upstream wind turbine. *Front Mar Sci* 2022;9:1039233. <https://doi.org/10.3389/fmars.2022.1039233>.
- [32] Tian W, Ozbay A, Hu H. An experimental investigation on the wake interferences among wind turbines sited in aligned and staggered wind farms. *Wind Energy* 2018;21:100–14. <https://doi.org/10.1002/we.2147>.
- [33] Wu C, Yang X, Zhu Y. On the design of potential turbine positions for physics-informed optimization of wind farm layout. *Renew Energy* 2021;164:1108–20. <https://doi.org/10.1016/j.renene.2020.10.060>.
- [34] Stevens RJAM, Martínez-Tossas LA, Meneveau C. Comparison of wind farm large eddy simulations using actuator disk and actuator line models with wind tunnel experiments. *Renew Energy* 2018;116:470–8. <https://doi.org/10.1016/j.renene.2017.08.072>.
- [35] Zhang M, Arendshorst MG, Stevens RJAM. Large eddy simulations of the effect of vertical staggering in large wind farms. *Wind Energy* 2019;22:189–204. <https://doi.org/10.1002/we.2278>.
- [36] Navarro Diaz GP, Otero AD, Asmuth H, Sørensen JN, Ivanell S. Actuator line model using simplified force calculation methods. *Wind Energy Sci* 2023;8:363–82. <https://doi.org/10.5194/wes-8-363-2023>.
- [37] Martínez-Tossas LA, Churchfield MJ, Leonardi S. Large eddy simulations of the flow past wind turbines: actuator line and disk modeling: LES of the flow past wind turbines: actuator line and disk modeling. *Wind Energy* 2015;18:1047–60. <https://doi.org/10.1002/we.1747>.
- [38] Chiang Y-C, Hsu Y-C, Chau S-W. Power prediction of wind farms via a simplified actuator disk model. *J Mar Sci Eng* 2020;8:610. <https://doi.org/10.3390/jmse8080610>.
- [39] Ravensbergen M, Bayram Mohamed A, Korobenko A. The actuator line method for wind turbine modelling applied in a variational multiscale framework. *Comput Fluids* 2020;201:104465. <https://doi.org/10.1016/j.compfluid.2020.104465>.
- [40] Nathan J, Masson C, Dufresne L. Near-wake analysis of actuator line method immersed in turbulent flow using large-eddy simulations. *Wind Energy Sci* 2018;3:905–17. <https://doi.org/10.5194/wes-3-905-2018>.
- [41] Xue F, Duan H, Xu C, Han X, Shangguan Y, Li T, et al. Research on the power capture and wake characteristics of a wind turbine based on a modified actuator line model. *Energies* 2022;15:282. <https://doi.org/10.3390/en15010282>.
- [42] Yuan Y, Hao H, Yu Z, Zheng X, Wang C. Experimental and numerical validation of a hybrid method for modelling the wake flow of two in-line wind turbines. *Eng Appl Comput Fluid Mech* 2023;17:2270505. <https://doi.org/10.1080/19942060.2023.2270505>.
- [43] Troldborg N, Sørensen JN, Mikkelsen R. Numerical simulations of wake characteristics of a wind turbine in uniform inflow. *Wind Energy* 2010;13:86–99. <https://doi.org/10.1002/we.345>.
- [44] Li N, Liu Y, Li L, Chang S, Han S, Zhao H, et al. Numerical simulation of wind turbine wake based on extended *k-epsilon* turbulence model coupling with actuator disc considering nacelle and tower. *IET Renew Power Gener* 2020;14:3834–42. <https://doi.org/10.1049/iet-rpg.2020.0416>.
- [45] Ti Z, Deng XW, Yang H. Wake modeling of wind turbines using machine learning. *Appl Energy* 2020;257:114025. <https://doi.org/10.1016/j.apenergy.2019.114025>.
- [46] Ti Z, Deng XW, Zhang M. Artificial Neural Networks based wake model for power prediction of wind farm. *Renew Energy* 2021;172:618–31. <https://doi.org/10.1016/j.renene.2021.03.030>.
- [47] Wu Y-T, Porté-Agel F. Large-eddy simulation of wind-turbine wakes: evaluation of turbine parametrisations. *Bound-Layer Meteorol* 2011;138:345–66. <https://doi.org/10.1007/s10546-010-9569-x>.
- [48] McKenna R, Pfenninger S, Heinrichs H, Schmidt J, Staffell I, Bauer C, et al. High-resolution large-scale onshore wind energy assessments: a review of potential definitions, methodologies and future research needs. *Renew Energy* 2022;182:659–84. <https://doi.org/10.1016/j.renene.2021.10.027>.
- [49] Bou-Zeid E, Meneveau C, Parlange M. A scale-dependent Lagrangian dynamic model for large eddy simulation of complex turbulent flows. *Phys Fluids* 2005;17:025105. <https://doi.org/10.1063/1.1839152>.
- [50] Calaf M, Meneveau C, Meyers J. Large eddy simulation study of fully developed wind-turbine array boundary layers. *Phys Fluids* 2010;22:015110. <https://doi.org/10.1063/1.3291077>.
- [51] VerHulst C, Meneveau C. Large eddy simulation study of the kinetic energy entrainment by energetic turbulent flow structures in large wind farms. *Phys Fluids* 2014;26:025113. <https://doi.org/10.1063/1.4865755>.
- [52] Stevens RJAM, Gayme DF, Meneveau C. Large eddy simulation studies of the effects of alignment and wind farm length. *J Renew Sustain Energy* 2014;6:023105. <https://doi.org/10.1063/1.4869568>.
- [53] VerHulst C, Meneveau C. Altering kinetic energy entrainment in large eddy simulations of large wind farms using unconventional wind turbine actuator forcing. *Energies* 2015;8:370–86. <https://doi.org/10.3390/en8010370>.
- [54] Wu Y-T, Porté-Agel F. Large-eddy simulation of wind-turbine wakes: evaluation of turbine parametrisations. *Bound-Layer Meteorol* 2011;138:345–66. <https://doi.org/10.1007/s10546-010-9569-x>.
- [55] Wu Y-T, Porté-Agel F. Simulation of turbulent flow inside and above wind farms: model validation and layout effects. *Bound-Layer Meteorol* 2013;146:181–205. <https://doi.org/10.1007/s10546-012-9757-y>.